Chapter 3

Supersymmetry and Models with Large Extra Dimensions

The Standard Model is in very good agreement with all confirmed experimental data from high-energy colliders. Despite its remarkable success, the Standard Model contains several conceptual problems and raises a number of open questions (see Section 2.1.3 of the previous chapter). Therefore, the majority of particle physicists believe that there is a theory which extends the Standard Model to higher energies and improves our understanding of the particle world.

In this chapter, I describe two of the most interesting extensions of the Standard Model, Supersymmetry and models with large extra dimensions. In particular, I will concentrate on how these theories could lead to an anomalous production of photonic events with missing energy. I will also discuss the search strategies for such signals at LEP.

3.1 Supersymmetry

3.1.1 Introduction

In 1928, Paul Dirac incorporated the symmetries of the Lorentz group into quantum mechanics [29]. As a natural consequence, he found that each known particle had to have a partner – an antiparticle. Matter-antimatter symmetry was not revealed until experimental tools were developed to detect positrons in cosmic rays [30]. In a similar manner, Supersymmetry (SUSY) predicts partner particles for all known particles [31]. The basic idea of SUSY models is the existence of fermionic charges

that relate bosons to fermions:

$$\hat{Q}|\text{fermion}>=|\text{boson}> \qquad \hat{Q}|\text{boson}>=|\text{fermion}>, \tag{3.1}$$

which in turn means that each Standard Model particle should have a SUSY *superpartner*. The new SUSY particles are then combined with their partner Standard Model particles into *supermultiplets*. Two particles of a supermultiplet have the same quantum numbers and couplings but differ by 1/2 unit of spin. For example, the superpartners of quarks and leptons are scalar particles called *squarks* and *sleptons* (for more details see Section 3.1.2).

Supersymmetry has become the dominant framework for formulating physics beyond the Standard Model. Perhaps the most compelling argument for the existence of Supersymmetry is that this is the last still undiscovered symmetry consistent with the relativistic quantum theory [32]. Furthermore, SUSY realizations near the electroweak scale (i.e., below or near 1 TeV) can be used to cure several of the shortcomings of the Standard Model, as I discuss below.

Hierarchy Problem

The main theoretical reason to expect SUSY at an accessible energy scale is provided by the *hierarchy* or *naturalness* problem of the Higgs mass. In the Standard Model, quantum loop corrections to the Higgs mass [33], illustrated by the one-loop diagrams in Figure 3.1a, are each quadratically divergent:

$$\delta M_H^2 \;=\; \mathcal{O}\left(\frac{g_2^2}{16\pi^2}\right)\int^{\Lambda} d^4k\frac{1}{k^2} \;=\; \mathcal{O}\left(\frac{\alpha}{\pi}\right)\Lambda^2\,, \tag{3.2}$$

where the cutoff Λ represents the scale where new physics beyond the Standard Model appears. If we assume that the Standard Model is valid all the way up to the Planck mass $M_{\rm P} \sim 10^{19}$ GeV, where gravity is expected to become as strong as other particle interactions, then the quantum corrections of Equation 3.2 will be 36 orders of magnitude greater than the physical values of $M_H \sim 100$ GeV [34]. In principle, this

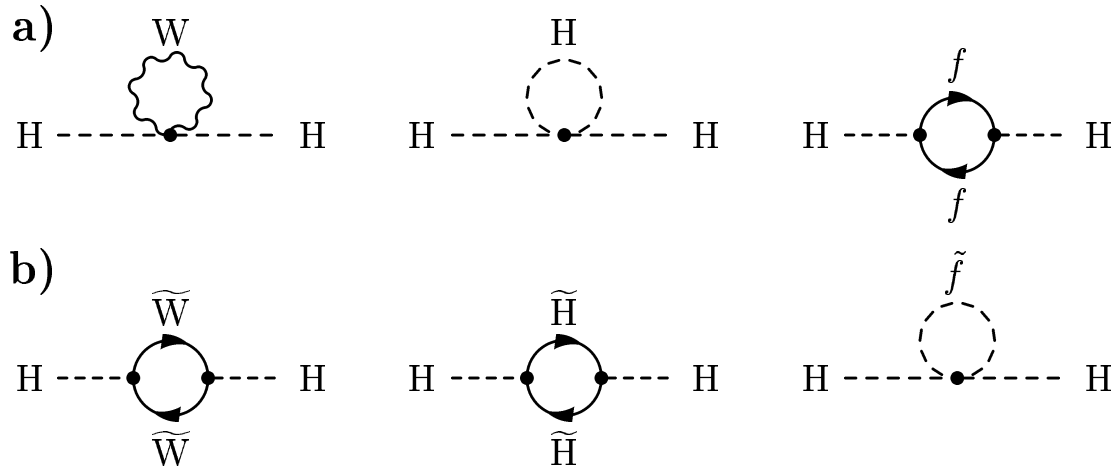

Figure 3.1: a) One-loop quantum corrections to M_H^2 in the Standard Model and b) the additional corrections in Supersymmetry.

is not a problem from the mathematical point of view in renormalization theory: one could postulate the tree-level value of the Higgs mass to be very large so that it would (almost) completely cancel the loop corrections and give us the correct physical value of M_H. However, this mechanism appears to be rather unnatural and one would prefer to keep the quantum corrections of the same order as the physical value of the Higgs mass.

This is possible in a supersymmetric theory, in which there are equal numbers of bosons (b) and fermions (f) with identical couplings. Since the contributions from the bosonic and fermionic loops have opposite signs (see Figure 3.1), the residual one-loop corrections become:

$$\delta M_H^2 = -\left(\frac{g_f^2}{16\pi^2}\right)\left(\Lambda^2 + m_f^2\right) + \left(\frac{g_b^2}{16\pi^2}\right)\left(\Lambda^2 + m_b^2\right) = \mathcal{O}\left(\frac{\alpha}{4\pi}\right)\left|m_b^2 - m_f^2\right|, \quad (3.3)$$

which is smaller than M_H^2 if the supersymmetric partners have similar masses:

$$\left|m_b^2 - m_f^2\right| \leq 1 \text{ TeV}^2. \quad (3.4)$$

This means that in order to keep the naturalness argument valid, masses of supersymmetric partner particles should be not much larger than 1 TeV.

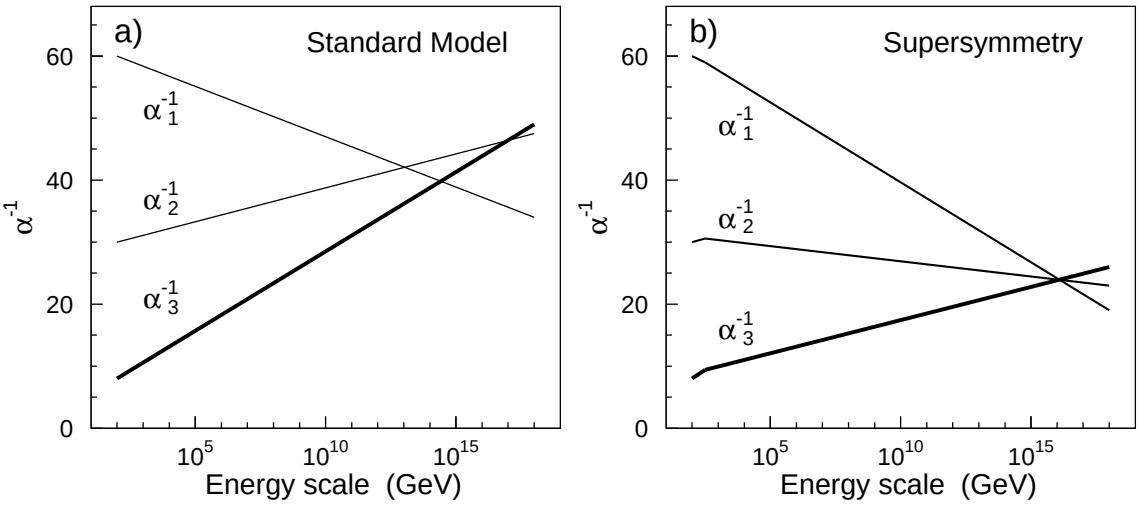

Figure 3.2: Evolution of the $SU(3)_C \times SU(2)_L \times U(1)_Y$ gauge couplings to high energy scales in the Standard Model a) and in Supersymmetry b).

Gauge Unification in SUSY

Another appealing feature of Supersymmetry at the weak scale is related to the effect it has on the running of the gauge couplings. In grand unification theories (GUTs), one assumes that there exists a unification of QCD and the electroweak sector of the Standard Model. In other words, the three inverse coupling constants ($1/\alpha_1$, $1/\alpha_2$, $1/\alpha_3$) of the electromagnetic, weak, and strong interactions converge and become equal at the unification energy scale. The coupling constants depend on the energy scale Q through loop corrections to the corresponding vertices and gauge bosons propagators [35], where the loops are generated by all particles with masses smaller than Q. Therefore, the evolution of the coupling constants is sensitive to the particle content of the theory.

In the Standard Model, the three couplings tend to approach each other at high energies, but fail to coincide at a single point, as shown in Figure 3.2a. However, the evolution graph will be changed if there exists Supersymmetry on the TeV scale. The loop corrections from the new SUSY particles start contributing above the energy scale $M_{\rm SUSY} \sim 1$ TeV, which produces a kink in the evolution of the coupling con-

stants.[1] Figure 3.2b shows that in this case the grand unification is indeed allowed and occurs at the unification scale of $U_{\mathrm{SUSY}} \sim 10^{16}$ GeV.

R–Parity

Supersymmetry opens the possibility of Lagrangian terms which explicitly violate lepton (L) and baryon (B) number conservation. However, if SUSY is realized on the TeV scale, then such $B-$ and $L-$violating interactions are severely restricted by the experimental measurements. For example, no evidence for fast proton decay has been observed, and the current lower bound on the proton lifetime is $\tau > 2.1 \times 10^{29}$ years at the 90% confidence level [6].

In order to forbid the lepton- and baryon-number violating terms, a new symmetry is introduced: *R–parity* [36]. For a particle of spin S, the R–parity is defined as

$$\mathrm{R} \;=\; (-1)^{3(B-L)+2S}. \tag{3.5}$$

This is a multiplicative quantum number, and all particles of the Standard Model have R–parity $+1$, while their superpartners (*sparticles*) have R–parity -1. The conservation of R–parity in scattering and decay processes has a crucial impact on the supersymmetric phenomenology:

- Sparticles can only be produced in pairs.
- Heavier sparticles decay into lighter ones.
- The lightest sparticle (LSP) is stable because it has no allowed decay modes.

Throughout this thesis the R–parity is assumed to be conserved.

The LSP must be neutral and colorless since there are stringent cosmological bounds on the existence of light stable particles which are electrically charged or strongly interacting [37]. As a consequence, the LSP in R–parity conserving SUSY models interacts with ordinary matter only by the exchange of a heavy virtual SUSY

[1] The masses of SUSY particles are assumed to be below or near M_{SUSY}.

particle and cannot be detected at collider experiments (much like a neutrino) [38]. Thus, a generic collider signature for R–parity conserving Supersymmetry is missing transverse momentum from the escaping LSPs.

Moreover, in such SUSY theories the LSP is a primary candidate for the non-baryonic dark matter, *Cold Dark Matter* [39], which is required in the current models of cosmology and galaxy formation [40]. Recent results from the WMAP experiment [41] suggest that more than 80% of the matter in our Universe consists of cold dark matter. Further aspects of the non-baryonic and supersymmetric dark matter can be found in Reference [42].

3.1.2 The Minimal Supersymmetric Standard Model

The simplest supersymmetric extension of the Standard Model is called the Minimal Supersymmetric Standard Model (MSSM). The particle spectrum of the MSSM consists of the Standard Model particles and their superpartners. In addition, the MSSM contains an extra Higgs doublet, giving a total of two doublets with hypercharge $Y = \pm 1$. In this way, flavor changing neutral currents[2] are avoided at tree level since the $Y = -1$ and $Y = +1$ doublets couple only to the "up"–type and "down"–type quarks (and charged leptons), respectively [44]. The particle content of the MSSM is listed in Table 3.1.

If supersymmetry was an exact symmetry of nature, then the Standard Model particles and their superpartners would be degenerate in mass and the sparticles would have been discovered long time ago. Thus, it is clear that a realistic SUSY theory must contain *supersymmetry breaking*. The most general way to introduce supersymmetry breaking is to add to the Lagrangian explicit *soft*[3] SUSY-breaking terms consistent with the symmetries of the Standard Model. The effective Lagrangian of the MSSM

[2] In the Standard Model with only one Higgs doublet, tree-level flavor changing neutral currents are automatically absent because the same operations that diagonalize the mass matrix automatically diagonalize the Higgs-fermion couplings [43].

[3] These interactions are referred to as soft because they do not re-introduce the quadratic divergences which motivated the introduction of Supersymmetry in the first place [45].

Particles	Supersymmetric partners			
	Weak interaction eigenstates		Mass eigenstates	
$l = \mathrm{e}, \mu, \tau$	$\tilde{l}_\mathrm{L}$, $\tilde{l}_\mathrm{R}$	Sleptons	$\tilde{l}_1, \tilde{l}_2$	
ν_l	$\tilde{\nu}_l$	Sneutrinos	$\tilde{\nu}_l$	
q = u, c, t / d, s, b	$\tilde{\mathrm{q}}_\mathrm{L}$, $\tilde{\mathrm{q}}_\mathrm{R}$	Squarks	$\tilde{\mathrm{q}}_1, \tilde{\mathrm{q}}_2$	
g	$\tilde{\mathrm{g}}$	Gluino	$\tilde{\mathrm{g}}$	
$\mathrm{W}^\pm$	$\widetilde{\mathrm{W}}^\pm$	Wino	$\tilde{\chi}^\pm_{1,2}$	Charginos
$\mathrm{H}^\pm$	$\widetilde{\mathrm{H}}^\pm$	Higgsinos		
γ	$\tilde{\gamma}$	Photino	$\tilde{\chi}^0_{1\ldots4}$	Neutralinos
Z	$\widetilde{\mathrm{Z}}$	Zino		
h, H, A	$\widetilde{\mathrm{H}}_{1,2}$	Higgsinos		
G	$\widetilde{\mathrm{G}}$	Gravitino	$\widetilde{\mathrm{G}}$	

Table 3.1: Particle content of the MSSM.

can then be written as a sum of SUSY-preserving and SUSY-breaking parts:

$$\mathcal{L} = \mathcal{L}_{SUSY} + \mathcal{L}_{soft}. \tag{3.6}$$

The resulting theory has more than 100 additional parameters which were not present in the Standard Model. The number of such parameters can be significantly reduced by making explicit assumptions about the nature of the supersymmetry breaking, as discussed in detail in Section 3.1.3.

Higgs in Supersymmetry

The extended Higgs sector of the MSSM contains two doublets. One of the doublets couples exclusively to "down"-type quarks and charged leptons and has a vacuum expectation value v_d, while the other couples only to "up"-type particles with a vacuum expectation value of v_u [43]. The squared sum of the their vacuum expectation

values is connected to the W boson mass through

$$v_d^2 + v_u^2 = v^2 = 4M_W^2/g^2 \simeq (246 \text{ GeV})^2, \tag{3.7}$$

while their ratio, traditionally written as

$$\tan\beta = \frac{v_u}{v_d}, \tag{3.8}$$

is a free parameter of the model. After the electroweak symmetry breaking, five physical Higgs particles remain in this model: a charged Higgs boson pair ($H^{\pm}$), two CP–even neutral Higgs bosons (h and H with $M_h \leq M_H$), and one CP–odd neutral Higgs boson (A). At tree level, the whole Higgs-sector is determined by two parameters, typically taken to be $\tan\beta$ and M_A [43].

It should be also noted that, at tree level, the MSSM predicts that the lightest neutral Higgs boson (h) should not be heavier than the Z boson, $M_h \leq M_Z$ [46]. However, this upper bound is somewhat weakened if one includes the quantum loop corrections. Current calculations yield $M_h \lesssim 130$ GeV [47], which implies that the MSSM Higgs boson should be observed at the LHC.

Neutralinos and Charginos

As a result of supersymmetry breaking, SUSY particles with the same quantum numbers are allowed to mix in a manner analogous to the mixing of the B and W^3 fields due to the electroweak symmetry breaking in the Standard Model (see Section 2.1.2). In particular, the superpartners of the Higgs and electroweak gauge bosons, higgsinos and gauginos, can mix with each other. The neutral higgsinos ($\widetilde{\mathrm{H}}_1$ and $\widetilde{\mathrm{H}}_2$) and the neutral gauginos ($\widetilde{\mathrm{B}}$ and $\widetilde{\mathrm{W}}^3$) combine to form four neutral mass eigenstates called neutralinos, $\tilde{\chi}^0_{1\ldots4}$. The charged higgsinos ($\widetilde{\mathrm{H}}^+$ and $\widetilde{\mathrm{H}}^-$) and the charged winos ($\widetilde{\mathrm{W}}^+$ and $\widetilde{\mathrm{W}}^-$) mix to form four charged eigenstates called charginos, $\tilde{\chi}^{\pm}_{1,2}$ (see Table 3.1). By convention these are labeled in ascending order with $m_{\tilde{\chi}^0_1} < m_{\tilde{\chi}^0_2} < m_{\tilde{\chi}^0_3} < m_{\tilde{\chi}^0_4}$ and $m_{\tilde{\chi}^{\pm}_1} < m_{\tilde{\chi}^{\pm}_2}$.

This mixing can be expressed using the following three parameters: M_1 and M_2 which correspond to the bino and wino mass terms in the SUSY-breaking part of Lagrangian $\mathcal{L}_{soft}$, and the Higgs mixing parameter μ. The physical chargino and neutralino masses can then be obtained by diagonalizing the mass mixing matrices

$$\mathcal{M}_{\tilde{\chi}^{\pm}} = \begin{pmatrix} M_2 & \sqrt{2}\mathrm{M_W}\sin\beta \\ \sqrt{2}\mathrm{M_W}\cos\beta & \mu \end{pmatrix} \tag{3.9}$$

for charginos and

$$\mathcal{M}_{\tilde{\chi}^0} = \begin{pmatrix} M_1 & 0 & -\mathrm{M_Z}\, s_\theta \cos\beta & \mathrm{M_Z}\, s_\theta \sin\beta \\ 0 & M_2 & \mathrm{M_Z}\, c_\theta \cos\beta & -\mathrm{M_Z}\, c_\theta \sin\beta \\ -\mathrm{M_Z}\, s_\theta \cos\beta & \mathrm{M_Z}\, c_\theta \cos\beta & 0 & -\mu \\ \mathrm{M_Z}\, s_\theta \sin\beta & -\mathrm{M_Z}\, c_\theta \sin\beta & -\mu & 0 \end{pmatrix} \tag{3.10}$$

for neutralinos, where $s_\theta \equiv \sin\theta_\mathrm{W}$, $c_\theta \equiv \cos\theta_\mathrm{W}$, and the mass matrix for neutralinos is given in the gauge-eigenstate basis ($\widetilde{\mathrm{B}}$,$\widetilde{\mathrm{W}}^3$,$\widetilde{\mathrm{H}}_1$,$\widetilde{\mathrm{H}}_2$) [48]. In general, the neutralino mass eigenstates do not correspond to a photino (a fermion partner of the photon) or a zino (a fermion partner of the Z boson), but are complicated mixtures of these states. The photino is a mass eigenstate only if $M_1 = M_2$. Physics involving the neutralinos therefore depends on M_1, M_2, μ, and $\tan\beta$ parameters.

In order to reduce the number of free parameters in the theory, a frequently used approach is to assume that the gaugino masses also unify at the GUT scale. In this case, the effective gaugino mass parameters are related to each other through:

$$M_1 = \frac{5}{3}\tan^2\theta_\mathrm{W}\, M_2\,, \qquad M_3 \equiv m_{\tilde{\mathrm{g}}} = \frac{\alpha_\mathrm{s}}{\alpha_\mathrm{em}}\sin^2\theta_\mathrm{W}\, M_2\,, \tag{3.11}$$

where M_3 is the mass parameter associated with $SU(3)_C$, $m_{\tilde{\mathrm{g}}}$ is the gluino mass, and M_1 and M_2 enter the neutralino and chargino mass matrices. Substituting the following parameter values $\alpha_S = 0.118$, $\alpha = 1/128$, and $\sin^2\theta_W = 0.23$, one finds

$$M_3 : M_2 : M_1 \approx 7 : 2 : 1 \tag{3.12}$$

at the electroweak scale. In particular, this means that the gluino should be much heavier than the lighter neutralinos and charginos [38].

Sfermions

The supersymmetric partners of the quarks and leptons are scalar bosons called squarks, charged sleptons, and sneutrinos. For a given fermion f, there are two supersymmetric partners $\tilde{f}_{\mathrm{L}}$ and $\tilde{f}_{\mathrm{R}}$, the superpartners for the two helicity states (left and right-handed) of this fermion.[4] In general, $\tilde{f}_{\mathrm{L}}$ and $\tilde{f}_{\mathrm{R}}$ are not mass eigenstates since they are allowed to mix. However, the strength of this mixing is proportional to the mass of the corresponding Standard Model partner and, hence, the mixing is expected to be negligibly small for the first two generations of sparticles. Only for the third generation is a substantially large mixing possible. In this case, the squark and slepton mass eigenstates are generically called $\tilde{f}_1$ and $\tilde{f}_2$.

3.1.3 Supersymmetry Breaking

As mentioned in the previous section, supersymmetry must be a broken symmetry. According to the Goldstone theorem [49], spontaneous breaking of any global symmetry gives rise to a massless Nambu-Goldstone mode with the same quantum numbers as the broken symmetry generator. In the case of supersymmetry, the broken generator is the fermionic charge Q and the Nambu-Goldstone particle must be a massless neutral fermion called the *goldstino*. The goldstino would then be the LSP and could play a role in SUSY phenomenology [50].

However, no satisfactory models of global supersymmetry breaking exist. Thus, the supersymmetry must be made a local symmetry. In this case, the goldstino is absorbed by the gravitino, the spin–3/2 superpartner of the graviton, which also acts as a gauge field [51]. The gravitino participates in the supersymmetric version of the

[4] There is no $\tilde{\nu}_{\mathrm{R}}$ in the MSSM.

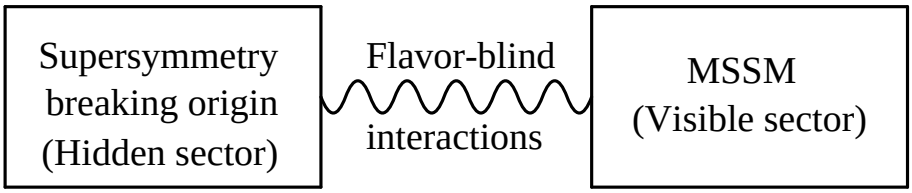

Figure 3.3: The presumed schematic structure of the supersymmetry breaking.

Higgs mechanism and acquires a non-zero mass

$$m_{\widetilde{\mathrm{G}}} \sim \frac{F}{M_{\mathrm{Pl}}}, \tag{3.13}$$

where $\sqrt{F}$ is the characteristic scale of the local supersymmetry breaking and M_{Pl} is the Planck mass [38].

Thus far no one has succeeded in crafting an acceptable model in which the supersymmetry breaking arises solely due to interactions between the MSSM particles. This problem is usually addressed by extending the MSSM to a new theory which holds two distinct sectors: a "hidden" sector built of particles with no direct couplings to the Standard Model gauge group and a "visible" sector containing the particles of the MSSM. There should be no tree-level interactions between particles of the visible and hidden sectors. It is assumed that supersymmetry breaking occurs in the hidden sector and is transmitted to the visible sector of the MSSM by some mechanism, as shown in Figure 3.3. Two theoretical scenarios have been examined in detail: *gravity-mediated* and *gauge-mediated* supersymmetry breaking.

Gravity-mediated SUSY Breaking

In the gravity-mediated SUSY breaking scenario (SUGRA), the mediating interactions between the hidden and visible sectors are assumed to be of gravitational nature [52, 53]. More precisely, they are assumed to be associated with some new physics, which includes gravity and enters at the Planck scale. In such models, the SUSY breaking scale is predicted to be of the order of 10^{11} GeV. The gravitino mass is then expected to be comparable to the masses of the MSSM sparticles, while its

couplings are of gravitational strength. Hence, it follows that the gravitino would not play any role in collider physics.

In the minimal SUGRA model,[5] the scalar quarks and leptons are assumed to have the same mass and the same trilinear couplings at the GUT scale [52]. With these universality conditions, the whole sparticle spectrum is determined by only five free parameters: M_2, μ, and $\tan\beta$, described in the previous section; the common scalar mass at the GUT scale m_0; and the common Higgs-sfermion-sfermion trilinear interaction parameter A at the GUT scale [54]. In R–parity conserving SUGRA models, the LSP is typically taken to be the lightest neutralino.

Gauge-mediated SUSY Breaking

In the gauge-mediated supersymmetry breaking scenario (GMSB), the supersymmetry breaking is assumed to be communicated to the visible sector by the ordinary electroweak and QCD gauge interactions The SUSY breaking again occurs in the hidden sector, however the splitting of masses in the MSSM sector is generated at some lower energy scale, in the "messenger sector," which contains pairs of heavy messenger quarks and leptons [55, 56]. The direct coupling of messengers to the hidden sector generates a supersymmetry breaking spectrum in the messenger sector. Gauge interactions then mediate supersymmetry breaking needed in the observable sector. In this scenario, the supersymmetry breaking scale $\sqrt{F}$ is expected to be between about 10 TeV and 100 TeV, and the gravitino mass is typically in the eV to keV range. The couplings of the gravitino to the other MSSM particles can become strong enough to let the gravitino play an important role in collider experiments.

Since the GMSB scenario can naturally lead to photonic signatures at LEP, let us discuss the MSSM spectrum in such models. The whole mass spectrum of the MSSM can be described by five free parameters of the model plus the gravitino mass [57]. The free GMSB parameters are the supersymmetry breaking scale in the messenger sector Λ, the messenger mass M_m, the messenger index N_m (an integer), $\tan\beta$, and sign(μ), where μ is the Higgs mixing parameter. Several examples of the MSSM

[5]The minimal SUGRA model is sometimes referred to as mSUGRA or constrained MSSM.

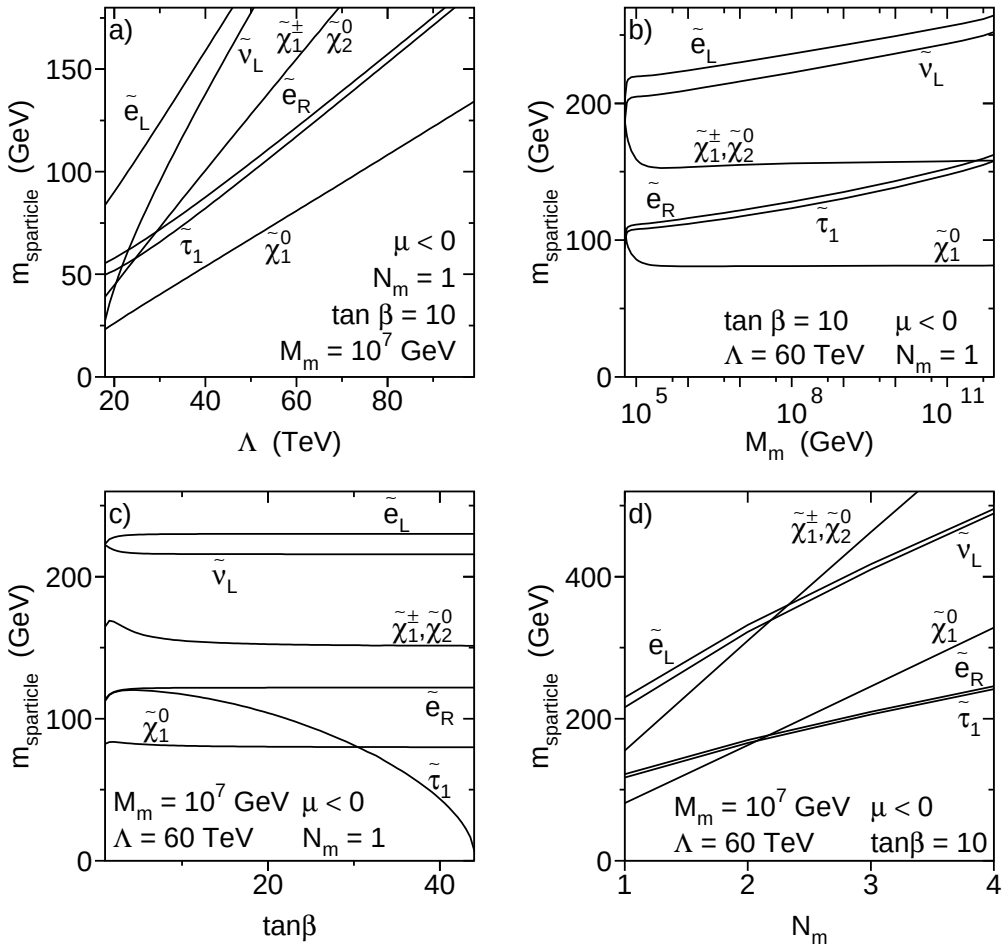

Figure 3.4: The masses of the sleptons and lightest gauginos as functions of the GMSB parameters Λ, M_m, $\tan\beta$, and N_m [58]. The values of the fixed parameters are indicated on the plots.

mass spectra are shown in Figure 3.4 for a broad range of the GMSB parameters, as calculated with the `ISASUSY` program [59]. A hierarchy between strongly interacting and weakly interacting particles holds throughout the whole parameter space keeping squarks much heavier than sleptons and the lightest gauginos.

The gravitino is always the LSP in the GMSB theories, while the next-to-lightest supersymmetric particle (NLSP) can either be the lightest neutralino $\tilde{\chi}_1^0$ or the lightest stau $\tilde{\tau}_1$ depending on the values of N_m, M_m, and $\tan\beta$ (see Figure 3.4). In this thesis, I will consider only the $\tilde{\chi}_1^0$ NLSP scenario because only such scenario could lead to an anomalous production of photonic events with missing energy at LEP.

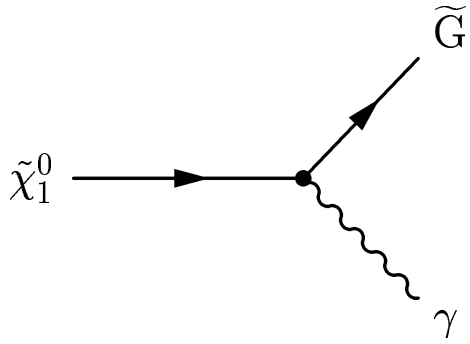

Figure 3.5: Feynman graph for the two-body neutralino decay $\tilde{\chi}_1^0 \to \gamma\tilde{\mathrm{G}}$.

The lightest neutralino is in general a mixture of the superpartners of the electroweak gauge and Higgs bosons, which can be conveniently parameterized as

$$\tilde{\chi}_1^0 = \sum_{i=1}^{4} N_i \psi_i^0 \,, \tag{3.14}$$

where $\psi^0 = (\tilde{\mathrm{B}}, \widetilde{\mathrm{W}}^3, \tilde{\mathrm{H}}_1, \tilde{\mathrm{H}}_2)$ is the gauge-eigenstate basis. In most cases of GMSB models, the lightest neutralino is almost pure bino,[6] $N_1 \simeq 1$, and decays predominantly into a gravitino and a photon, $\tilde{\chi}_1^0 \to \gamma\tilde{\mathrm{G}}$ (see Figure 3.5) [56]. The corresponding decay width is given by [60]

$$\Gamma(\tilde{\chi}_1^0 \to \gamma\tilde{\mathrm{G}}) = \frac{\kappa_\gamma}{48\pi} \frac{m_{\tilde{\chi}_1^0}^5}{m_{\mathrm{Pl}}^2 m_{\tilde{\mathrm{G}}}^2} \,, \tag{3.15}$$

where $\kappa_\gamma = |N_1 \cos\theta_{\mathrm{W}} + N_2 \sin\theta_{\mathrm{W}}|^2$ gives the photino component of the neutralino and $m_{\mathrm{Pl}} = M_{\mathrm{Pl}}/\sqrt{8\pi} \approx 2.4 \cdot 10^{18}$ GeV is the reduced Planck mass. The Planck-scale suppression $m_{\tilde{\chi}_1^0}^2/m_{\mathrm{Pl}}^2$ is compensated by the factor $m_{\tilde{\chi}_1^0}^2/m_{\tilde{\mathrm{G}}}^2$, which gives a sizable decay width. In the rest frame of the decaying neutralino, the photons and gravitinos are produced isotropically with an energy equal to $m_{\tilde{\chi}_1^0}/2$ (for kinematic purposes the gravitino mass can be ignored).

It should be noted that sufficiently heavy neutralinos can also decay into a Z boson

[6] Bino is the superpartner of B, the gauge boson of the $U(1)_Y$ group of the Standard Model.

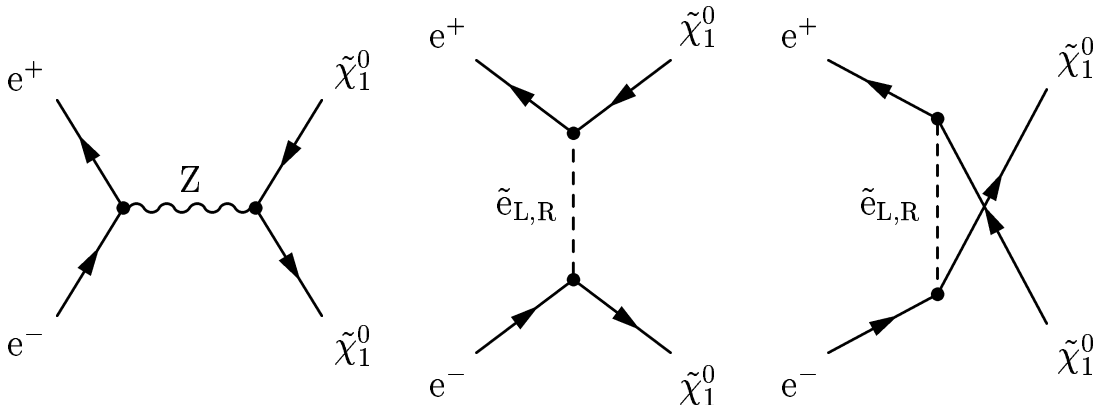

Figure 3.6: Feynman diagrams for the neutralino pair-production at LEP.

and a gravitino. However, this decay mode is strongly suppressed:

$$\frac{\Gamma(\tilde{\chi}_1^0 \to \mathrm{Z}\tilde{\mathrm{G}})}{\Gamma(\tilde{\chi}_1^0 \to \gamma\tilde{\mathrm{G}})} = \frac{\kappa_\mathrm{Z}}{\kappa_\gamma}\left(1 - \frac{M_Z^2}{m_{\tilde{\chi}_1^0}^2}\right)^4, \tag{3.16}$$

where $\kappa_\mathrm{Z} = |N_{11}\sin\theta_\mathrm{W} + N_{12}\cos\theta_\mathrm{W}|^2 + \frac{1}{2}|N_{13}\cos\beta - N_{14}\sin\beta|^2$. If the neutralino is pure bino, $\kappa_\mathrm{Z}/\kappa_\gamma \simeq 0.3$. Complete expressions for the neutralino decay rates into three-body final states ($\tilde{\chi}_1^0 \to \tilde{\mathrm{G}}f\bar{f}$) can be found in Reference [61].

3.2 Single- and Multi-Photon Signatures in SUSY

Different SUSY models may lead to different single- or multi-photon with missing energy signatures. In this section, I will describe the possible signal topologies, discuss my motivation for searching for such signals at LEP, and outline the search strategies that I will later use in Chapter 7.

3.2.1 Neutralino Production in GMSB

Neutralinos can be pair-produced in $\mathrm{e^+e^-}$ collisions by Z exchange in the s–channel or by scalar electron exchange in the t– and u–channels [62]. The Feynman diagrams of this process are shown in Figure 3.6. As discussed in the previous section, I consider

the GMSB scenario where the massless (for kinematic purposes) gravitino is the LSP and the lightest neutralino is the NLSP and almost pure bino. Since only the higgsino components of the neutralino directly couple to the Z boson, the s–channel contribution is negligible. The cross section of this reaction is an incoherent sum of contributions from the right- and left-handed selectron exchange diagrams[7] and is given by [64]

$$\frac{d\sigma}{d\cos\theta} = \sum_{i=\tilde{e}_R,\tilde{e}_L} \frac{\beta^3}{s}\frac{\pi\alpha Y_i^4}{2\cos^4\theta_W} \times \Big[\frac{1-\cos^2\theta}{(1+\Delta M_i)^2-\beta^2\cos^2\theta} + \frac{2\Delta M_i^2\cos^2\theta}{[(1+\Delta M_i^2)^2-\beta^2\cos^2\theta]^2}\Big], \tag{3.17}$$

where $\sqrt{s}$ is the center-of-mass energy, θ is the polar angle, $\beta = \sqrt{1-4m^2_{\tilde{\chi}^0_1}/s}$ is the neutralino velocity in the laboratory frame, $\Delta M_i = 2\cdot(m_i^2 - m^2_{\tilde{\chi}^0_1})/s$, and Y_i is the hypercharge of the right- and left-selectrons ($Y_{\tilde{e}_R} = -2$ and $Y_{\tilde{e}_L} = -1$). Because the selectron hypercharge is to the fourth power and the left-selectron is usually heavier than the right-selectron, it is clear that the dominant contributions come from the $\tilde{e}_R$ exchange.

For given values of the neutralino mass and center-of-mass energy, the production cross section depends only on the selectron mass. In GMSB models, the ratio $m_{\tilde{e}_R}/m_{\tilde{\chi}^0_1}$ cannot become larger than about 1.5 [65]. Thus, the $e^+e^- \to \tilde{\chi}^0_1\tilde{\chi}^0_1$ cross section cannot be smaller than a certain minimum value. Figure 3.7 shows the maximum and minimum cross section values as a function of the neutralino mass. This cross section range was obtained with the following scan over the GMSB parameter space:

$$\begin{aligned} 10\text{ TeV} \le\ & \Lambda && \le 100\text{ TeV} \\ \Lambda/0.9 \le\ & M_m && \le \Lambda/0.01 \\ & N_m && = 1,2,3,4 \\ 1 \le\ & \tan\beta && \le 60 \\ & \operatorname{sign}\mu && = \pm, \end{aligned} \tag{3.18}$$

[7] The two selectrons $\tilde{e}_R$ and $\tilde{e}_L$ do not mix, and the interference between the right and left-handed selectron exchange diagrams is suppressed by a factor of $\mathcal{O}(m_e/m_{\tilde{e}})$ and hence is negligible [63].

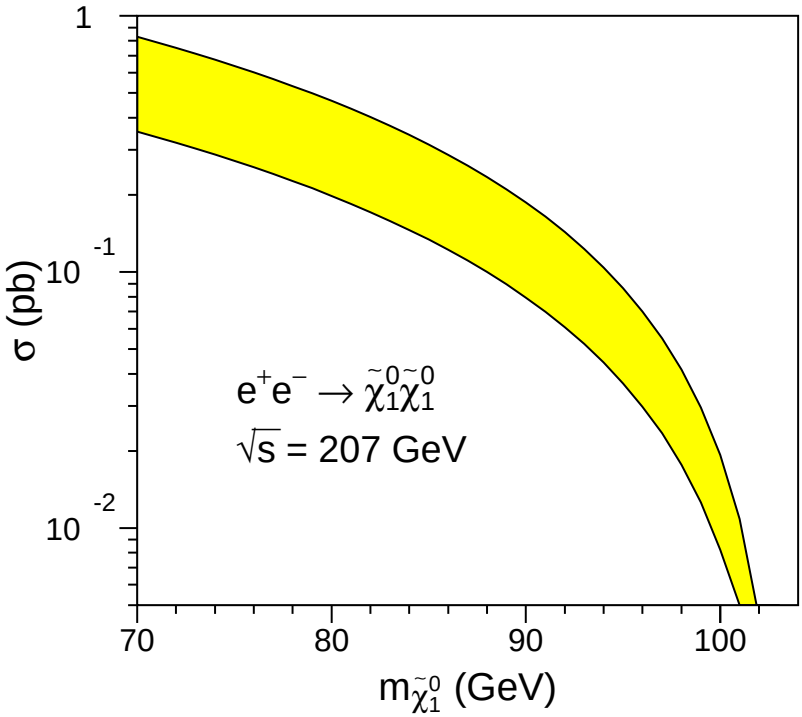

Figure 3.7: Cross section range for the reaction $e^+e^- \to \tilde{\chi}_1^0\tilde{\chi}_1^0$ at $\sqrt{s}$ = 207 GeV, as a function of the mass of the lightest neutralino in GMSB models.

where the parameter ranges that I used were defined in Reference [65]. Sparticle masses and couplings are calculated from the GMSB model parameters using the `ISASUSY` program [59], which has been interfaced to the `SUSYGEN` Monte Carlo generator [66] to derive the neutralino pair-production cross section, including initial-state radiation. Figure 3.7 shows that for any values of the GMSB parameters, the reaction $e^+e^- \to \tilde{\chi}_1^0\tilde{\chi}_1^0$ has a sizable cross section almost up to the kinematic limit of $m_{\tilde{\chi}_1^0} = \sqrt{s}/2$.

As discussed in the previous section, the produced neutralinos decay predominantly into a gravitino and a photon. Because the gravitinos would escape undetected, the reaction $e^+e^- \to \tilde{\chi}_1^0\tilde{\chi}_1^0 \to \tilde{G}\tilde{G}\gamma\gamma$ would lead to two photons and missing energy in the final state. Each of the neutralinos is produced with an energy equal to the beam energy, $E_{\tilde{\chi}_1^0} = \sqrt{s}/2$, and decays isotropically. Thus, the photon energies

have a flat distribution in the range $E_{\min} < E_{\gamma_1}, E_{\gamma_2} < E_{\max}$ with

$$E_{\max,\min} = \frac{1}{4}\left(\sqrt{s} \pm \sqrt{s - 4m^2_{\tilde{\chi}^0_1}}\right) . \tag{3.19}$$

In order to investigate the kinematic distributions of the final-state photons, I used the SUSYGEN program to generate samples of 300,000 MC events for three different values of the neutralino mass: $m_{\tilde{\chi}^0_1} = 55, 75, 95$ GeV. The event samples were generated at $\sqrt{s} = 200$ GeV which corresponded to the typical center-of-mass energy of LEP2. Figures 3.8a,c show that the photon energy spectrum is indeed flat. The corresponding distributions of the polar angle ($\cos\theta_\gamma$) and the recoil mass are shown in Figures 3.8b,d, where the event recoil mass was defined in Section 2.2.2, Equation 2.23. The distribution of the photon polar angle is also almost flat.[8]

In this search channel, the main background comes from the Standard Model process $e^+e^- \to \nu\bar{\nu}\gamma\gamma$ (see Section 2.2.2). However, by comparing Figures 3.8 and 2.10 one can see that the kinematic distributions of the signal are very different from those of the background. In particular, the energy of the second photon is expected to be much higher for the signal than for the background. Moreover, the photons from the reaction $e^+e^- \to \nu\bar{\nu}\gamma\gamma$ are expected to be produced predominantly at low polar angles. Thus, an almost complete suppression of the background can be achieved with quite loose cuts on the E_{γ_2} and $\cos\theta_\gamma$ variables.

It should be noted that for certain values of the GMSB parameters the neutralino decay length can become non-negligible. The probability that a neutralino with energy $\sqrt{s}/2$ will travel a distance $\leq x$ in the laboratory frame before decaying is given by

$$P(x) = 1 - \exp(-x/L) . \tag{3.20}$$

[8] The neutralino production angle is not severely peaked (see Equation 3.17), and the decay $\tilde{\chi}^0_1 \to \tilde{G}\gamma$ is isotropic. Hence, the photon polar angle in the laboratory frame has a distribution very close to isotropic.

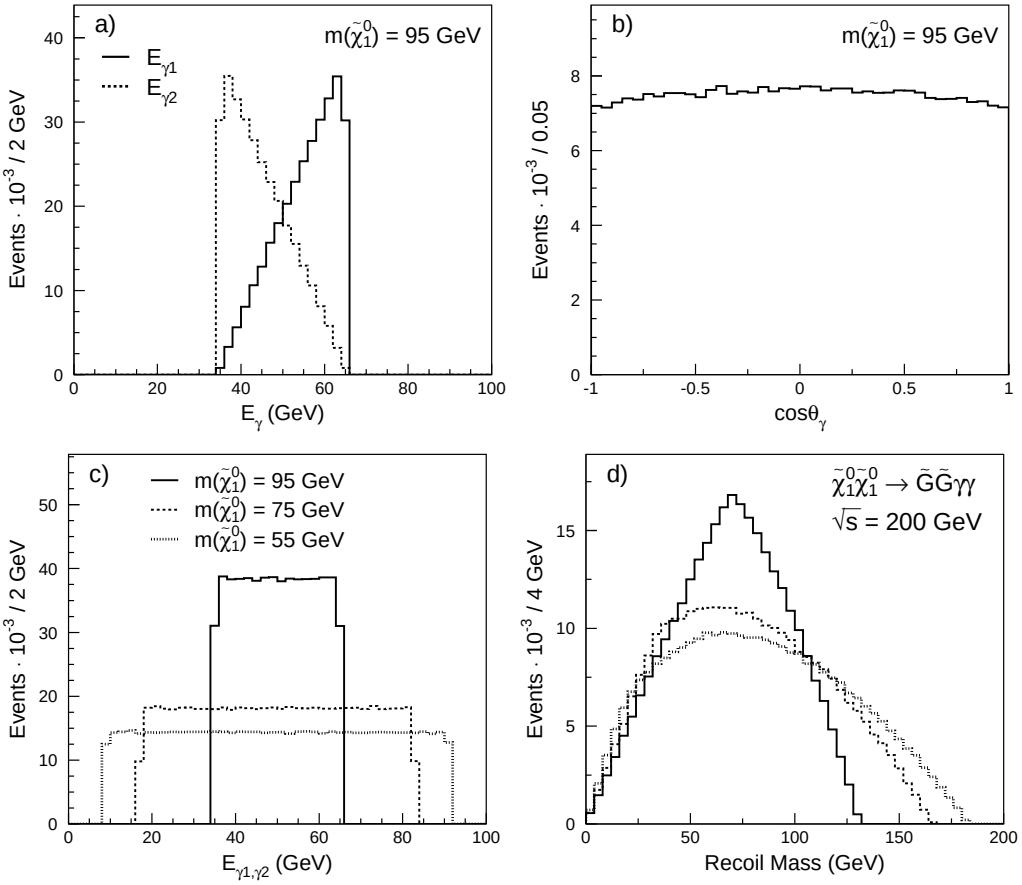

Figure 3.8: Kinematic distributions for the reaction $e^+e^- \to \tilde{\chi}_1^0\tilde{\chi}_1^0 \to \tilde{G}\tilde{G}\gamma\gamma$ at $\sqrt{s} = 200$ GeV, with arbitrary normalization. The distributions of a) $E_{\gamma_1}, E_{\gamma_2}$ and b) $\cos\theta_\gamma$ are shown for $m_{\tilde{\chi}_1^0} = 95$ GeV. Also shown are c) the photon energy and d) the recoil mass spectra, for various values of $m_{\tilde{\chi}_1^0}$.

The decay length L can be calculated using Equation 3.15 and expressed as [60]

$$L \;=\; 1.76 \cdot 10^{-3}\,(\kappa_\gamma)^{-1} \left(\frac{s}{4m^2_{\tilde{\chi}_1^0}} - 1\right)^{1/2} \left(\frac{100\ \text{GeV}}{m_{\tilde{\chi}_1^0}}\right)^5 \left(\frac{m_{\tilde{\mathrm{G}}}}{1\ \text{eV}}\right)^2 \text{cm}\,, \tag{3.21}$$

where, due to the dominantly bino nature of the neutralino, $(\kappa_\gamma)^{-1} \simeq 1.3$. For instance, for $\sqrt{s} = 200$ GeV, $m_{\tilde{\chi}_1^0} = 80$ GeV, and $m_{\tilde{\mathrm{G}}} = 200$ eV the neutralino decay length is approximately 2 m. In this case, the majority the neutralinos would decay inside the detector, away from the beam vertex.

As I will show in Chapter 7, the efficiency of the usual multi-photon selection drops significantly for decay lengths larger than about 10 cm. In order to investigate

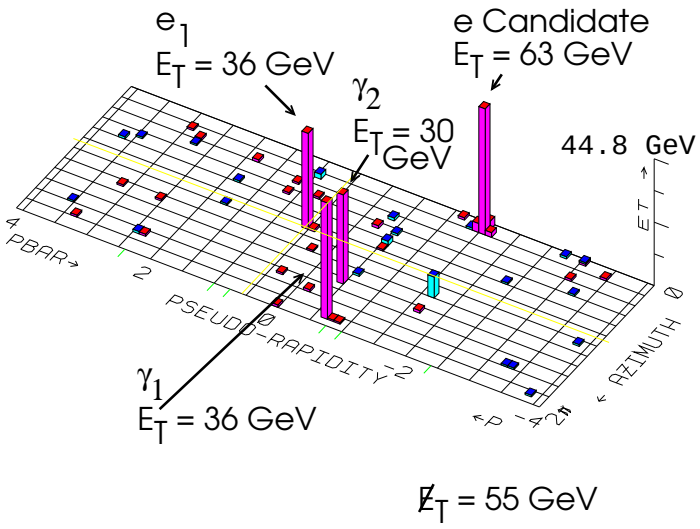

Figure 3.9: The ee$\gamma\gamma$ event observed by the CDF experiment [67].

the region of intermediate decay lengths, $0.1\,\mathrm{m} \lesssim L \lesssim 100\,\mathrm{m}$, I developed a new event selection which was able to identify *non-pointing* photons, i.e., photons not originating from the primary event vertex.

3.2.2 The CDF Event

In 1995, the CDF experiment at the Tevatron $p\bar{p}$ collider observed an event with two high-energy electrons, two high-energy photons, and a large amount of missing transverse energy (see Figure 3.9) [67]. There is no obvious explanation for this event in the Standard Model. The only Standard Model process able to produce such ee$\gamma\gamma$ events consists of the WW$\gamma\gamma$ production, where each W boson decays into an electron and a neutrino. However, the event rate from this process is expected to be very low and has been estimated by the CDF collaboration to be $(1 \pm 1) \cdot 10^{-6}$ events in their data sample corresponding to $85\,\mathrm{pb}^{-1}$ [67].

As a consequence, this unusual event generated a lot of interest among particle theorists, resulting in a publication of dozens of papers with various interpretations in models with physics beyond the Standard Model. In particular, this event has brought wide attention to photonic signatures in SUSY.

In GMSB models, this event is a candidate for the process $q\bar{q} \rightarrow \tilde{e}_R^+ \tilde{e}_R^-$ with subsequent decays $\tilde{e}_R^\pm \rightarrow e^\pm \tilde{\chi}_1^0$ and $\tilde{\chi}_1^0 \rightarrow \tilde{G}\,\gamma$, where the neutralinos and gravitinos escape detection.[9] Regions kinematically allowed for the CDF event correspond to 85 GeV $< m_{\tilde{e}_R} <$ 135 GeV and 50 GeV $< m_{\tilde{\chi}_1^0} <$ 100 GeV [68]. This means that the reaction $e^+e^- \rightarrow \tilde{\chi}_1^0\tilde{\chi}_1^0 \rightarrow \tilde{G}\tilde{G}\gamma\gamma$ could provide an excellent opportunity for SUSY discovery at LEP. This reaction was examined in the previous section.

The CDF event has also been interpreted in neutralino LSP models [69]. Again, the selectron pair-production in $q\bar{q}$ collisions can be the origin of this event, with the selectrons decaying into an electron and a $\tilde{\chi}_2^0$, and the $\tilde{\chi}_2^0$ then decaying radiatively to $\tilde{\chi}_1^0$. Within this framework, the event can only be accommodated in models with relaxed GUT boundary conditions for the gaugino mass parameters (see Equation 3.11). If this is the explanation for the CDF event, the best possibility for SUSY discovery at LEP is the reaction $e^+e^- \rightarrow \tilde{\chi}_2^0\tilde{\chi}_2^0 \rightarrow \tilde{\chi}_1^0\tilde{\chi}_1^0\gamma\gamma$. This reaction is examined in the next section.

In conclusion, searches for photonic events from the neutralino-pair production at LEP were highly motivated by the above interpretations of the CDF event.

3.2.3 Neutralino Production in SUGRA

In SUGRA models, the appearance of photonic final states with missing energy is possible only in the scenario where the R–parity is conserved, the next-to-lightest neutralino $\tilde{\chi}_2^0$ is the NLSP, and the lightest neutralino $\tilde{\chi}_1^0$ is the LSP. Moreover, the radiative decay $\tilde{\chi}_2^0 \rightarrow \tilde{\chi}_1^0\gamma$ should be the dominant decay mode. This decay mode is usually suppressed since it is a one-loop process (see Figure 3.10). In most SUSY scenarios, the next-to-lightest neutralino decays predominantly via $\tilde{\chi}_2^0 \rightarrow \tilde{\chi}_1^0 f\bar{f}$ through an exchange of a virtual sfermion or a Z boson.

As discussed in Section 3.1.2, the neutralinos are in general a superposition of the neutral gauginos and higgsinos. The couplings of sfermions to neutralinos involve only the gaugino component, while the Z boson couples only to the higgsino

[9] Chargino production also provides a possible explanation: $q\bar{q} \rightarrow \tilde{\chi}_1^+\tilde{\chi}_1^-$ with the decays $\tilde{\chi}_1^\pm \rightarrow e^\pm\,\nu_e\,\tilde{\chi}_1^0$ and $\tilde{\chi}_1^0 \rightarrow \tilde{G}\,\gamma$.

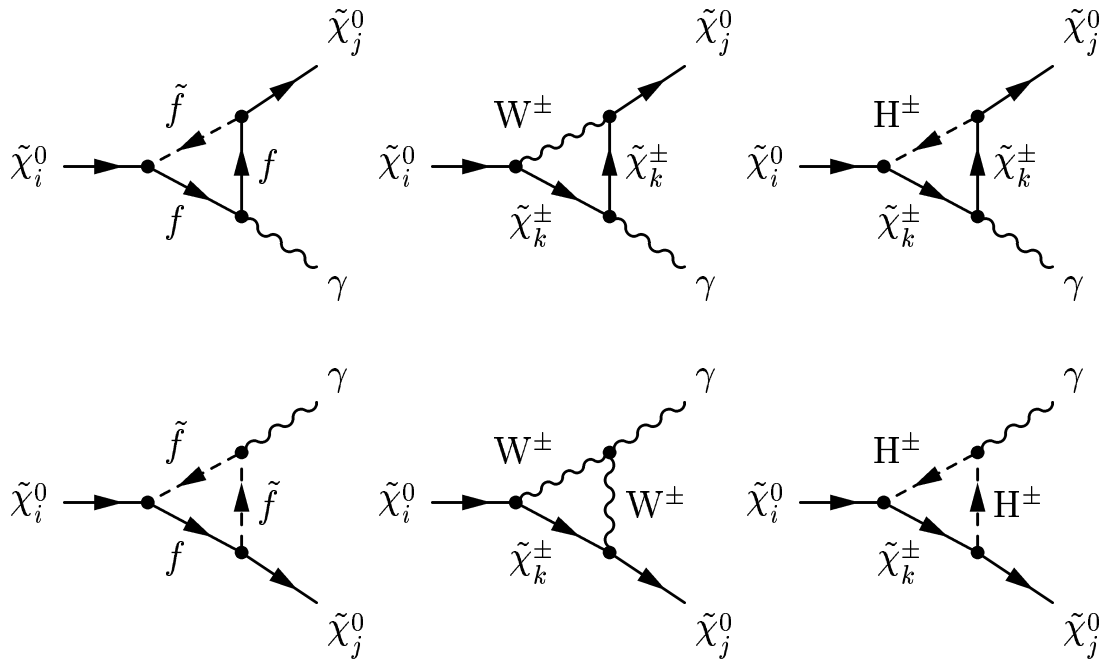

Figure 3.10: Feynman graphs for the radiative neutralino decay $\tilde{\chi}^0_2 \to \tilde{\chi}^0_1\gamma$.

component [70]. Hence, the tree-level decays $\tilde{\chi}^0_2 \to \tilde{\chi}^0_1 f\bar{f}$ require either simultaneous gaugino components in both neutralinos for the sfermion exchange process or simultaneous higgsino components for the Z exchange process. The above condition is not needed for the radiative decay, where both the gaugino and the higgsino components of neutralinos may be involved (apart from the two graphs on the left-hand side of Figure 3.10). Therefore, whenever the lightest neutralino is mainly higgsino and the next-to-lightest neutralino is mainly gaugino, the tree level $\tilde{\chi}^0_2$ width for the direct three-body decay is reduced and the radiative decay $\tilde{\chi}^0_2 \to \tilde{\chi}^0_1\gamma$ is enhanced.

It should be noted that this scenario is allowed only in a limited region of the MSSM parameter space [70]. However, it is favored by the SUGRA interpretation of the CDF event [69]. In particular, this scenario implies that the next-to-lightest neutralino is almost pure photino, $\tilde{\chi}^0_2 \simeq \tilde{\gamma}$, and the lightest neutralino is almost pure higgsino, $\tilde{\chi}^0_1 \simeq \tilde{\mathrm{H}}_b$, where $\tilde{\mathrm{H}}_b = \sin\beta\,\tilde{\mathrm{H}}_1 + \cos\beta\,\tilde{\mathrm{H}}_2$. In this case, the radiative decay $\tilde{\chi}^0_2 \to \tilde{\chi}^0_1\gamma$ is expected to have a branching ratio of almost 100%.

In this SUGRA scenario, the pair-production of neutralinos $\mathrm{e^+e^-} \to \tilde{\chi}^0_2\tilde{\chi}^0_2$ with a

subsequent decay $\tilde{\chi}_2^0 \to \tilde{\chi}_1^0\gamma$ leads to events with two photons and missing energy (due to the escaping neutralinos). The production mechanism and event topology are very similar to those of the GMSB process $e^+e^- \to \tilde{\chi}_1^0\tilde{\chi}_1^0 \to \tilde{G}\tilde{G}\gamma\gamma$, which was described in Section 3.2.1. Again, the dominant contributions come from the t– and u–channel $\tilde{e}_{R,L}$ exchange diagrams, and the radiative decay of the neutralino is isotropic in its rest frame. For a given center-of-mass energy, the $e^+e^- \to \tilde{\chi}_2^0\tilde{\chi}_2^0$ cross section depends only on the neutralino and selectron masses and is given by [63]

$$\frac{d\sigma}{d\cos\theta} = \sum_{i=\tilde{e}_R,\tilde{e}_L} \frac{\pi\alpha^2 s\beta^3}{4}\Big[\Big(\Delta M_i^2 + \frac{s}{2}\Big)^2 - \frac{s^2\beta^2}{4}\cos^2\theta\Big]^{-2} \times \Big[\frac{s^2\beta^2}{4}\cos^4\theta - s\Big[2\Big(\Delta M_i^2 + \frac{s}{2}\Big) - m_{\tilde{\chi}_2^0}^2 - \frac{s}{4}\Big]\cos^2\theta + \Big(\Delta M_i^2 + \frac{s}{2}\Big)^2\Big(1+\cos^2\theta\Big)\Big], \quad (3.22)$$

where $\sqrt{s}$ is the center-of-mass energy, θ is the polar angle, $\beta = \sqrt{1 - 4m_{\tilde{\chi}_2^0}^2/s}$ is the neutralino velocity in the laboratory frame, and $\Delta M_i = m_i^2 - m_{\tilde{\chi}_2^0}^2$. The pair-produced neutralinos are photino-like so that their couplings to the left- and right-selectrons are identical. This means that for $m_{\tilde{e}_R} = m_{\tilde{e}_L}$, the contributions from the $\tilde{e}_R$ and $\tilde{e}_L$ exchange diagrams are the same.

The photon energy and angular distributions have the same flat shape as the distributions from the GMSB reaction $e^+e^- \to \tilde{\chi}_1^0\tilde{\chi}_1^0$ (see Figure 3.8). However, in this case the lightest neutralino cannot be assumed to be massless, so that the expression for the kinematically allowed range of the photon energy needs to modified as

$$E_{\max,\min} = \frac{E_{\tilde{\chi}_2^0}}{2}\left(1 \pm \sqrt{1 - \frac{m_{\tilde{\chi}_2^0}^2}{E_{\tilde{\chi}_2^0}^2}}\right)\frac{m_{\tilde{\chi}_2^0}^2 - m_{\tilde{\chi}_1^0}^2}{m_{\tilde{\chi}_2^0}^2}, \quad (3.23)$$

where $E_{\tilde{\chi}_2^0} = \sqrt{s}/2$. Because the event topologies for the SUGRA and GMSB processes ($e^+e^- \to \tilde{\chi}_2^0\tilde{\chi}_2^0$ and $\tilde{\chi}_1^0\tilde{\chi}_1^0$) are essentially the same, for this signal I will use the same search strategy that I described in Section 3.2.1.

Neutralino production in SUGRA can also lead to a single-photon event topology via the reaction $e^+e^- \to \tilde{\chi}_2^0\tilde{\chi}_1^0$ with a subsequent decay $\tilde{\chi}_2^0 \to \tilde{\chi}_1^0\gamma$ [62]. However, for the photino-like $\tilde{\chi}_2^0$ and higgsino-like $\tilde{\chi}_1^0$, the cross section for this process is expected

to be extremely low [64]. Nevertheless, I will search for this reaction in the context of the model-independent search $e^+e^- \rightarrow XY \rightarrow YY\gamma$, where X and Y are new neutral invisible particles. As above, the photon energy and angular distributions are flat, and the kinematically allowed range of the photon energy is given by Equation 3.23, where the neutralino energy is $E_{\tilde{\chi}_2^0} = (s + m^2_{\tilde{\chi}_2^0} - m^2_{\tilde{\chi}_1^0})/(2\sqrt{s})$.

3.2.4 The Reactions $e^+e^- \rightarrow \tilde{\chi}_1^0\widetilde{G}$ and $e^+e^- \rightarrow \widetilde{G}\widetilde{G}\gamma$

In Section 3.1.3 I discussed models with gauge-mediated supersymmetry breaking, where the LSP is the gravitino with a mass in the eV to keV range. Such light gravitinos can also arise in other SUSY models.

Even without any assumptions about the mechanism of supersymmetry breaking, the mass of the gravitino would still be coupled to the scale of local supersymmetry breaking by Equation 3.13. When the scale of local supersymmetry breaking is decoupled from the breaking of global supersymmetry, as in no-scale supergravity models [71], the gravitino can become *superlight* (10^{-6} eV $\lesssim m_{\widetilde{G}} \lesssim 10^{-4}$ eV) and can be produced not only in decays of SUSY particles but also directly, either in pairs [72] or associated with a neutralino [68, 73]. The process $e^+e^- \rightarrow \tilde{\chi}_1^0\tilde{\chi}_1^0 \rightarrow \widetilde{G}\widetilde{G}\gamma\gamma$ can also be interpreted [74] in terms of the MSSM model parameters M_2, μ and $\tan\beta$, which were introduced in Section 3.1.2.

No-scale supergravity becomes especially predictive in a model with flipped SU(5) gauge symmetry [75], where only one free parameter is needed to determine the whole mass spectrum of the MSSM except the gravitino mass [68]. This model was proposed by Lopez, Nanopoulos, and Zichichi, and is traditionally referred to as the LNZ model. Figure 3.11 shows that in the LNZ model the lightest neutralino is usually the NLSP. Phenomenologically, this model is the same as the neutralino LSP scenario in GMSB except that the gravitino mass is several orders of magnitude smaller and the neutralino always decays at the event vertex.

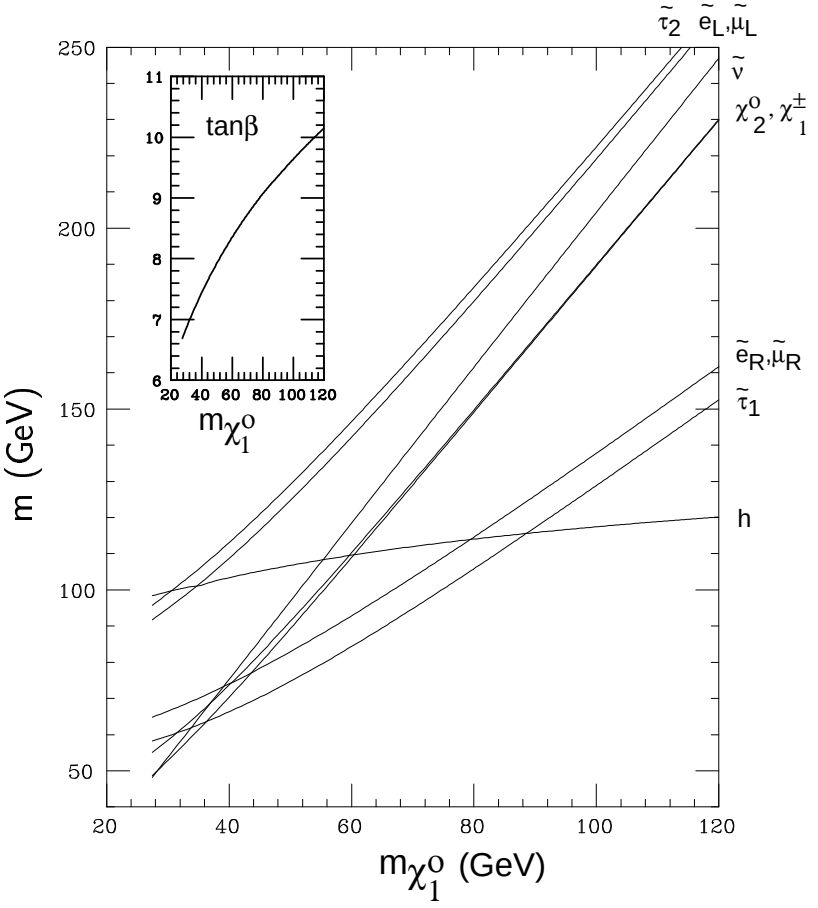

Figure 3.11: Masses of the lighter MSSM particles in the LNZ model versus the neutralino mass. The inset shows the variation of $\tan\beta$ with $m_{\tilde{\chi}^0_1}$ [68].

$\tilde{\chi}^0_1\widetilde{G}$ Production

The reaction $e^+e^- \to \tilde{\chi}^0_1\tilde{G} \to \tilde{G}\tilde{G}\gamma$ would lead to events with a single photon and missing energy in the final state. The Feynman diagrams of this process are shown in Figure 3.12. This reaction is expected have a sizable event rate at LEP2 only for very light gravitinos, $m_{\tilde{G}} \lesssim 10^{-4}$ eV, since its cross section scales as the inverse of the gravitino mass squared [73]. Thus, this process does not play a role in GMSB models where the gravitino is much heavier (see Section 3.1.3).

Due to the bino-like nature of the neutralino, the radiative decay $\tilde{\chi}^0_1 \to \tilde{G}\gamma$ is always the dominant decay mode. However, if the neutralino is heavier than the Z boson, the contribution of the decay into the Z needs to be taken into account. For

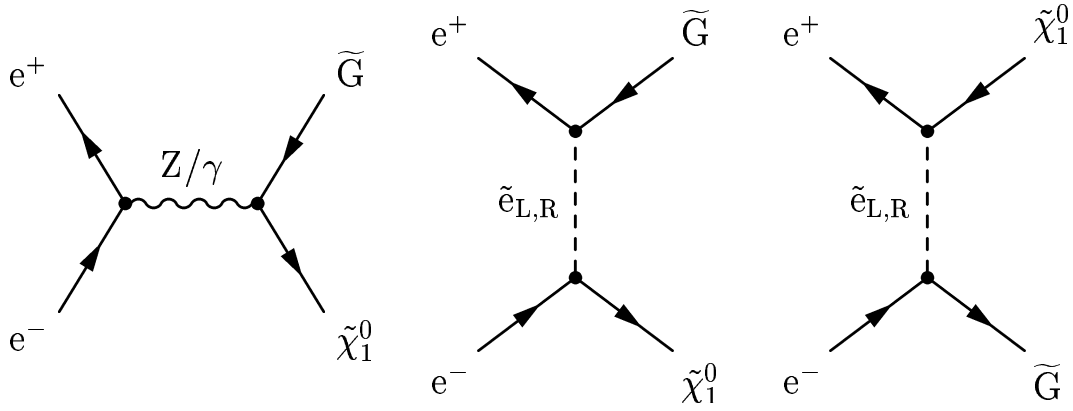

Figure 3.12: Feynman diagrams for the reaction $e^+e^- \to \tilde{\chi}_1^0\tilde{G}$.

instance, if $m_{\tilde{\chi}_1^0} = 200$ GeV, the branching ratio of the decay $\tilde{\chi}_1^0 \to \tilde{G}Z$ is equal to about 10% (see Equations 3.15 and 3.16).

In order to investigate the kinematic distributions of this process, I used samples of 300,000 MC events generated with the `SUSYGEN` program for two different values of the neutralino mass, $m_{\tilde{\chi}_1^0} = 150, 180$ GeV, at $\sqrt{s} = 200$ GeV, which corresponded to the typical center-of-mass energy of LEP2. Figure 3.13 shows that the resulting distributions of the photon energy and the cosine of the polar angle are again almost flat, where the kinematically allowed range for the photon energy is given by

$$\frac{m^2_{\tilde{\chi}_1^0}}{2\sqrt{s}} < E_\gamma < \frac{\sqrt{s}}{2}\,. \tag{3.24}$$

In this search channel, the principal background comes from the Standard Model process $e^+e^- \to \nu\bar{\nu}\gamma$ (see Section 2.2.2) whose differential cross sections are also shown in Figure 3.13. The kinematic distributions of the signal are very different from those of the background. For a large fraction of signal events, the photon energy is expected above the Z-return peak of the reaction $e^+e^- \to \nu\bar{\nu}\gamma$, where the Standard Model background is expected to be very low. Thus, a clean separation of the signal from the background can be achieved by an appropriate lower cut on the photon energy.

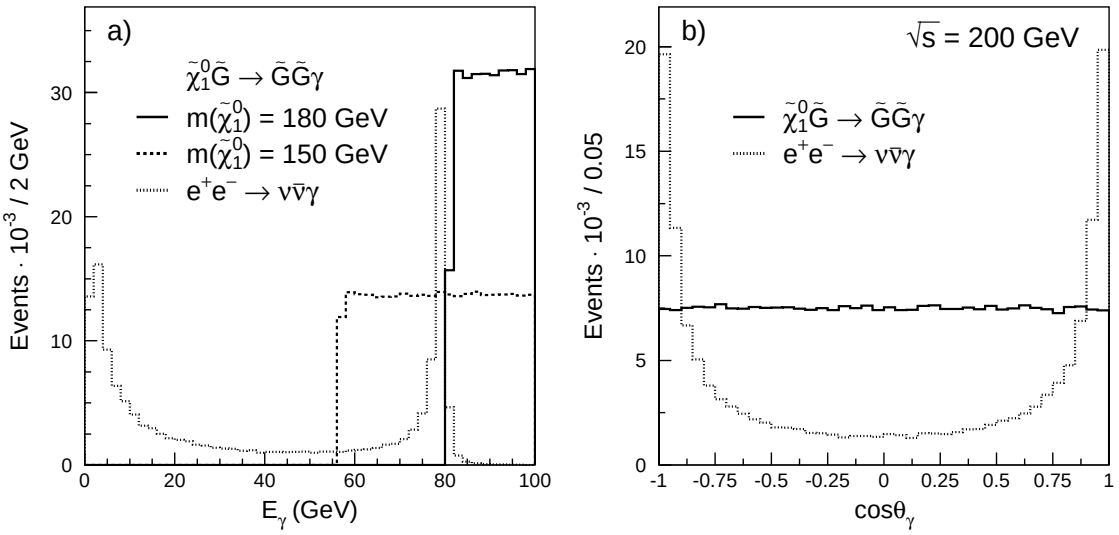

Figure 3.13: Distributions of a) the photon energy and b) the photon polar angle for the reaction $e^+e^- \to \tilde{\chi}_1^0\tilde{G} \to \tilde{G}\tilde{G}\gamma$ at $\sqrt{s} = 200$ GeV. Also shown are the corresponding distributions for the dominant background process $e^+e^- \to \nu\bar{\nu}\gamma$ with arbitrary normalization.

Gravitino Pair-Production

If the masses of all other SUSY particles are greater than the center-of-mass energy available at LEP, then the superlight gravitinos could still be detected via the reaction $e^+e^- \to \tilde{G}\tilde{G}\gamma$ [72, 76]. This process proceeds predominantly via initial-state radiation in the gravitino pair-production process, and its differential cross section is given by [72]

$$\frac{d^2\sigma}{dx_\gamma\, d\cos\theta_\gamma} = \left(\frac{\alpha {G_N}^2}{45}\right) \frac{s^3}{m_{\tilde{G}}^4}\, f(x_\gamma, \theta_\gamma)\,, \tag{3.25}$$

where G_N is the gravitational constant, $m_{\tilde{G}}$ is the gravitino mass, x_γ is the photon scaled energy $(E_\gamma/E_{\rm beam})$, θ_γ is the polar angle, and

$$f(x,\theta) = 2(1-x)^2 \left[\frac{(1-x)(2-2x+x^2)}{x\sin^2\theta} + \frac{x(-6+6x+x^2)}{16} - \frac{x^3\sin^2\theta}{32}\right]. \tag{3.26}$$

The production cross section depends only on one SUSY parameter – the gravitino mass. The photon energy spectrum is expected to be soft, as shown in Figure 3.14. Unfortunately, the dominant background process $e^+e^- \to \nu\bar{\nu}\gamma$ also proceeds via initial-

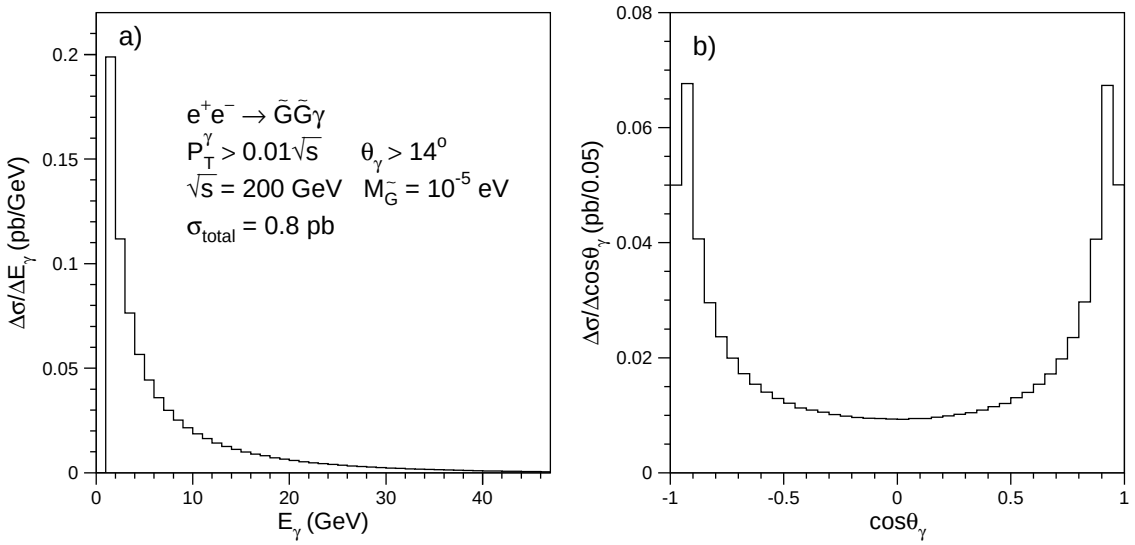

Figure 3.14: Differential cross sections of the reaction $e^+e^- \to \tilde{G}\tilde{G}\gamma$ as functions of a) the photon energy and b) $\cos\theta_\gamma$, calculated for $\sqrt{s} = 200$ GeV and $m_{\tilde{G}} = 10^{-5}$ eV.

state radiation, and its kinematic distributions are expected to be similar to those of the signal[10] (see Figures 2.8 and 2.7 in Section 2.2.2). Therefore, a clean separation of the signal from the background is not possible for this search channel.

3.2.5 Summary

In this section I briefly summarize the photonic SUSY signatures and the corresponding theoretical models. Common to all scenarios I considered are the requirements that the R–parity is conserved and that the lightest supersymmetric particle is colorless and electrically neutral (see Section 3.1). Two distinct signatures are investigated: events with a single photon plus missing energy and events with two photons plus missing energy in the final state. Several SUSY models predict processes that could lead to such signals at LEP.

Three SUSY processes could yield the single-photon signature: $\tilde{\chi}_1^0\tilde{\chi}_2^0$ production in SUGRA models where the neutralino is the LSP (see Section 3.2.3) and $\tilde{\chi}_1^0\tilde{G}$ and $\tilde{G}\tilde{G}\gamma$ production in models with superlight gravitinos, such as no-scale SUGRA

[10] The differential cross section of the signal does not have the Z-return peak.

Signature	Process	Decay	Model
$\gamma + E_{\rm miss}$	$\tilde{\chi}_1^0\tilde{\chi}_2^0$	$\tilde{\chi}_2^0 \to \tilde{\chi}_1^0\gamma$	SUGRA [62]
	$\tilde{\chi}_1^0\tilde{\rm G}$	$\tilde{\chi}_1^0 \to \tilde{\rm G}\gamma$	no-scale SUGRA, LNZ [68, 73]
	$\tilde{\rm G}\tilde{\rm G}\gamma$	—	no-scale SUGRA [72]
$\gamma\gamma + E_{\rm miss}$	$\tilde{\chi}_2^0\tilde{\chi}_2^0$	$\tilde{\chi}_2^0 \to \tilde{\chi}_1^0\gamma$	SUGRA [62]
	$\tilde{\chi}_1^0\tilde{\chi}_1^0$	$\tilde{\chi}_1^0 \to \tilde{\rm G}\gamma$	GMSB [65]
			no-scale SUGRA [73]

Table 3.2: Summary of the single- and multi-photon signatures in SUSY.

(see Section 3.2.4). The $\tilde{\chi}_1^0\tilde{\rm G}$ process can also be interpreted in the framework of the LNZ model, which is a more restrictive no-scale SUGRA model. An additional requirement needs to be imposed for the $\tilde{\rm G}\tilde{\rm G}\gamma$ process — all other SUSY particles have to be heavier than the center-of-mass energy [72].

The two-photon signature can arise from two similar reactions: $\tilde{\chi}_2^0\tilde{\chi}_2^0$ production in neutralino LSP models (see Section 3.2.3) and $\tilde{\chi}_1^0\tilde{\chi}_1^0$ production in gravitino LSP models (see Section 3.2.1). Searches for both these reactions at LEP are highly motivated by supersymmetric interpretations of the unusual event observed by the CDF experiment (see Section 3.2.2). The first process can be discussed in terms of the SUGRA model parameters introduced in Section 3.1.3. The second process is predicted by GMSB and no-scale SUGRA models (Sections 3.1.3 and 3.2.4). In GMSB models, the lightest neutralino can have a macroscopic decay length, which requires a special selection for photons not originating from the primary event vertex.

The photonic signatures and the corresponding SUSY processes and models are summarized in Table 3.2. The Standard Model background for these final-state topologies comes from the neutrino pair-production process accompanied by one or more photons from initial-state radiation, $\rm e^+e^- \to \nu\bar{\nu}\gamma(\gamma)$. Usually this background process can be almost completely suppressed using simple cuts on the photon energy and polar angle (see Sections 3.2.1 and 3.2.4). The only exception is the reaction $\rm e^+e^- \to \tilde{G}\tilde{G}\gamma$, where the signal cannot be separated from the Standard Model background.

3.3 Models with Large Extra Dimensions

The large disparity between the weak scale ($M_{\text{weak}} \sim 10^2$ GeV) and the traditional scale of gravity given by the Planck scale ($M_{\text{Pl}} \sim 10^{19}$ GeV) is considered to be one of the major theoretical problems in elementary particle physics. The origin of this large gap, as well as its stability under quantum corrections, demands explanation. This is known as the *hierarchy problem* of the Standard Model. The hierarchy problem can be successfully cured by introducing supersymmetry at the weak scale, as described in Section 3.1. Below I discuss another class of theories that are capable of addressing the hierarchy problem, models with *large extra dimensions* [77].

These models assume that the Standard Model fields, including ourselves, are confined to a four-dimensional hypersurface (brane) inside the full space-time (bulk), whereas the gravitational fields are also allowed to propagate in n extra spatial dimensions. We currently have almost no knowledge of gravity at distances less than about a millimeter since direct tests of Newton's law are based on torsion-balance experiments that are mechanically limited [78, 79]. Hence, it is conceivable that gravity may behave differently at small scales.

However, Newton's law must be reproduced at large distances so that gravity must behave as if there were only three spatial dimensions for $r \gtrsim 1\,\text{mm}$. In the ADD scenario[11] this is achieved by compactifying the extra dimensions on circles, where the geometry of these dimensions is flat and the topology is that of a torus.

The fundamental gravitational scale M_D is then related to the Planck scale through

$$M_{\text{Pl}}^2 \sim M_D^{2+n} R^n, \tag{3.27}$$

where R is the radius of the extra dimensions. Thus, the fundamental scale of gravity can be lowered to the TeV range while the size of the compactified extra dimensions can be as large as a millimeter. The radius of the compactified extra dimensions (R) can be expressed as a function of the parameters M_D and n. Assuming compactifi-

[11] This scenario was originally proposed by Arkani-Hamed, Dimopoulos, and Dvali in 1998 [77].

cation on a torus, this relationship is given by [80]

$$G_N^{-1} = 8\pi R^n M_D^{n+2}, \tag{3.28}$$

where G_N^{-1} is Newton's constant of gravitation. The case of one extra spatial dimension is thus ruled out since for $M_D \sim$ TeV, it would alter Newton's law at distances comparable to the size of the solar system.

Extra spatial dimensions could manifest themselves at present and future colliders in a variety of ways [78]. In particular, in e^+e^- collisions they could lead to the single-photon and missing energy signature in processes involving production of gravitons and branons. Below I give a brief description of these processes.

3.3.1 Graviton-Photon Production

In the framework of large extra dimensions, gravitational fields propagating in the bulk can be expressed as a series of states known as a Kaluza-Klein tower. For an observer trapped on the brane, these graviton modes appear as massive spin-2 neutral particles (G) that can couple to the Standard Model fields on the brane. As a result, real gravitons can be produced in e^+e^- collisions through the direct emission of a graviton and a photon, $e^+e^- \rightarrow \gamma G$ [80, 81]. The produced graviton behaves as if it was a massive, stable, and non-interaction particle and thus appears as missing energy in the detector. As shown in Figure 3.15, this process is expected to proceed through s–channel photon exchange, t–channel electron exchange, and four-particle contact interactions [81].

The differential cross section of this process depends on both the M_D and n [80]:

$$\frac{d^2\sigma\,(e^+e^- \rightarrow \gamma G)}{dx_\gamma\, d\cos\theta_\gamma} = \frac{\alpha}{32s}\frac{\pi^{n/2}}{\Gamma(n/2)}\left(\frac{\sqrt{s}}{M_D}\right)^{n+2} f(x_\gamma, \cos\theta_\gamma)\,, \tag{3.29}$$

where x_γ is the ratio of the photon energy to the beam energy, θ_γ is the polar angle

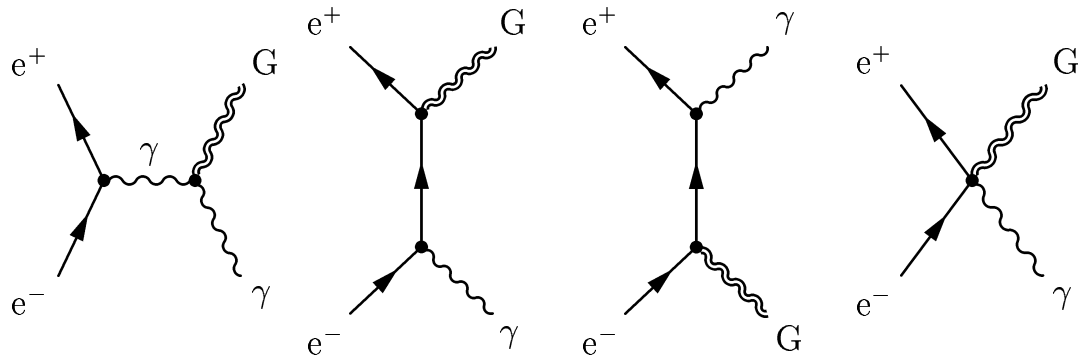

Figure 3.15: The lowest-order Feynman diagrams for the emission of a real graviton and a photon.

of the photon, α is the QED coupling, and the function $f(x, y)$ is given by

$$f(x,y) \;=\; \frac{2(1-x)^{\frac{n}{2}-1}}{x(1-y^2)}\left[(2-x)^2(1-x+x^2) - 3y^2x^2(1-x) - y^4x^4\right]. \qquad (3.30)$$

Figure 3.16 shows that the differential cross section increases rapidly at low photon energies and polar angles, where it scales as $(E_\gamma \sin^2\theta_\gamma)^{-1}$. The principal Standard Model background for this reaction comes from the process $e^+e^- \to \nu\bar{\nu}\gamma$, whose cross section also behaves as $\sim (E_\gamma \sin^2\theta_\gamma)^{-1}$ in the region of low E_γ and θ_γ (see Section A.1). Therefore, the graviton-photon signal cannot be separated from the $\nu\bar{\nu}\gamma$ background and can only be detected as an excess of events with one soft photon.

3.3.2 Branon Pair-Production in e^+e^- Collisions

A different theoretical scenario may also be considered. In this approach, the three-dimensional brane is treated as an additional physical body in the theory with its own dynamics. This may lead to the appearance of additional degrees of freedom corresponding to brane fluctuations along the extra-space dimensions, which would manifest themselves as new stable particles called *branons* ($\tilde{\pi}$) [82]. Their dynamics are determined by an effective theory with couplings of the same order as the brane tension (f). It should be noted that branons are natural dark-matter candidates [83] (see the discussion on dark-matter in Section 3.1).

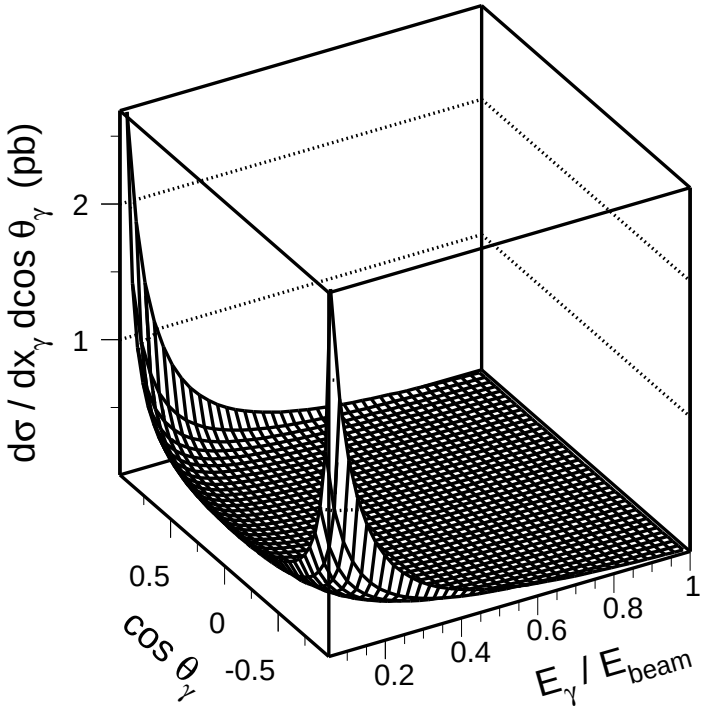

Figure 3.16: Differential cross section of the $e^+e^- \to \gamma G$ process, computed for $n = 2$, $M_D = 1.5$ TeV, and $\sqrt{s} = 207$ GeV.

Branons couple to the Standard Model particles in pairs and can be detected in e^+e^- collisions via the reaction $e^+e^- \to \tilde{\pi}\tilde{\pi}\gamma$. The Feynman diagrams of this process are shown in Figure 3.17. The final-state branons do not interact in the detector and are hence invisible. Thus, the experimental signature of the branon-photon production is the presence of a single photon together with missing energy. The differential cross section of this process is given by [84]

$$\frac{d^2\sigma\,(e^+e^- \to \tilde{\pi}\tilde{\pi}\gamma)}{dx_\gamma\, d\cos\theta_\gamma} = \frac{a_0 \alpha s}{f^8 \pi^2} \left(s(1-x_\gamma) - 4M^2\right)^2 \sqrt{1 - \frac{4M^2}{s(1-x_\gamma)}} \times \left[x_\gamma(3 - 3x_\gamma + 2x_\gamma^2) - x_\gamma^3 \sin^2\theta_\gamma + \frac{2(1-x_\gamma)(1+(1-x_\gamma)^2)}{x_\gamma \sin^2\theta_\gamma}\right], \tag{3.31}$$

where f is the brane tension, M is the branon mass,[12] $a_0 \equiv 1/61440$, and x_γ and θ_γ are the scaled energy and the polar angle of the photon ($x_\gamma = E_\gamma / E_{beam}$). The

[12]For simplicity, I consider a scenario with only one light branon species of mass M.

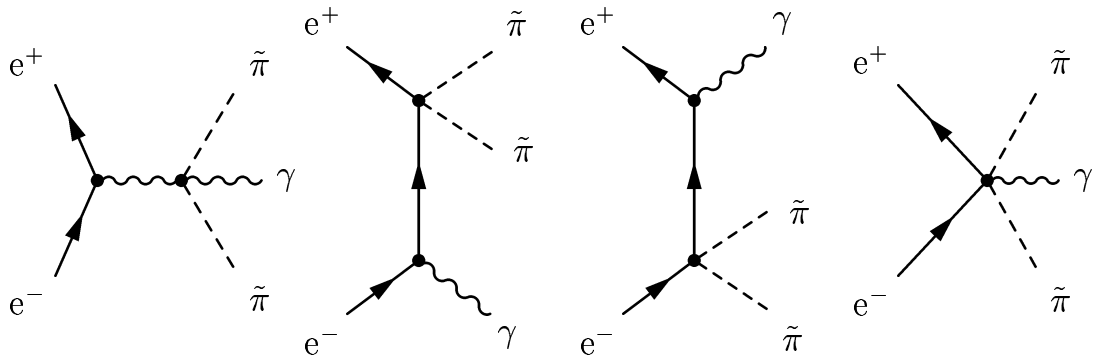

Figure 3.17: Feynman diagrams for the reaction $e^+e^- \to \tilde{\pi}\tilde{\pi}\gamma$.

kinematic properties of this signal are similar to those of the graviton-photon emission $e^+e^- \to \gamma G$, which was described in the previous section.

Searches for gravitons and branons are in a sense complementary [85]. If the brane tension is above the effective scale of gravity, $f \gg M_D$, the first evidence for extra dimensions would be the discovery of gravitons, giving information about the gravity scale and the number of extra spatial dimensions. If the brane tension is below the gravity scale, $f \ll M_D$, then the first signal of extra dimensions would be the discovery of branons, allowing a measurement of the brane tension scale, the number of branon species, and their masses [84].